Science Advances

AAAS

advances.sciencemag.org/cgi/content/full/4/2/eaao4350/DC1

Supplementary Materials for

Coral reef structural complexity provides important coastal protection from waves under rising sea levels

Daniel L. Harris, Alessio Rovere, Elisa Casella, Hannah Power, Remy Canavesio, Antoine Collin, Andrew Pomeroy, Jody M. Webster, Valeriano Parravicini

Published 28 February 2018, *Sci. Adv.* **4**, eaao4350 (2018)
DOI: 10.1126/sciadv.aao4350

This PDF file includes:

from CRIOBE and Moorea LTER (*4*) measurements (long-term) for each reef site.

- table S1. Sources of bathymetric data sets for Moorea and Tahiti.
- References (*58*, *59*)

Description of model scenarios and results

Six scenarios were simulated under different conditions of sea level and Reef Health Index (RHI) (fig. S1 and Fig. 1 in manuscript). Three primary scenarios, P1-3, are reported in the manuscript with the additional three supplementary scenarios (S1-3) reported in fig. S2. The supplementary scenarios were run to assess the changes in wave dissipation under additional scenarios of reef health index (defined in Fig. 1 of the manuscript) and sea level. The main conclusions from all six scenarios can be presented by focusing on scenarios P1-3 and as such, these scenarios are discussed in the manuscript. The descriptions below are organized with respect to the sea level inputs for each scenario. These scenarios are illustrated in fig. S1 and simulated wave transformation across coral reefs under the following conditions:

- P1 and S1 examined wave height changes at present sea level under different RHI (fig. S1 and Fig. 1 in the manuscript). P1 simulated wave conditions on a degraded reef with a low RHI and S2 a reef system at present sea level undergoing fluctuations of structural complexity reflecting the erosion and recovery of coral reefs before and after events such as cyclones or coral bleaching. S2 may also be a reef system that is keeping pace with sea level since in this instance relative sea level on the reef flats will not change.

- P2 and S2 add IPCC RCP4.5 sea level rise predictions to the P1 and S2 scenarios respectively (fig. S1).

- P3 and S3 are the full model simulations using the complete ranges of predicted sea level by 2100 under the RCP4.5 and 8.5 emissions scenarios respectively and the potential changes in structural complexity and vertical reef accretion or erosion (fig. S1). For our simulations P3 represents the most likely wave conditions in the future.

The results for the six scenarios at each reef site is shown in fig. S2. The average results for scenarios P1-3 from all reef sites is shown Fig. 2 in the manuscript.

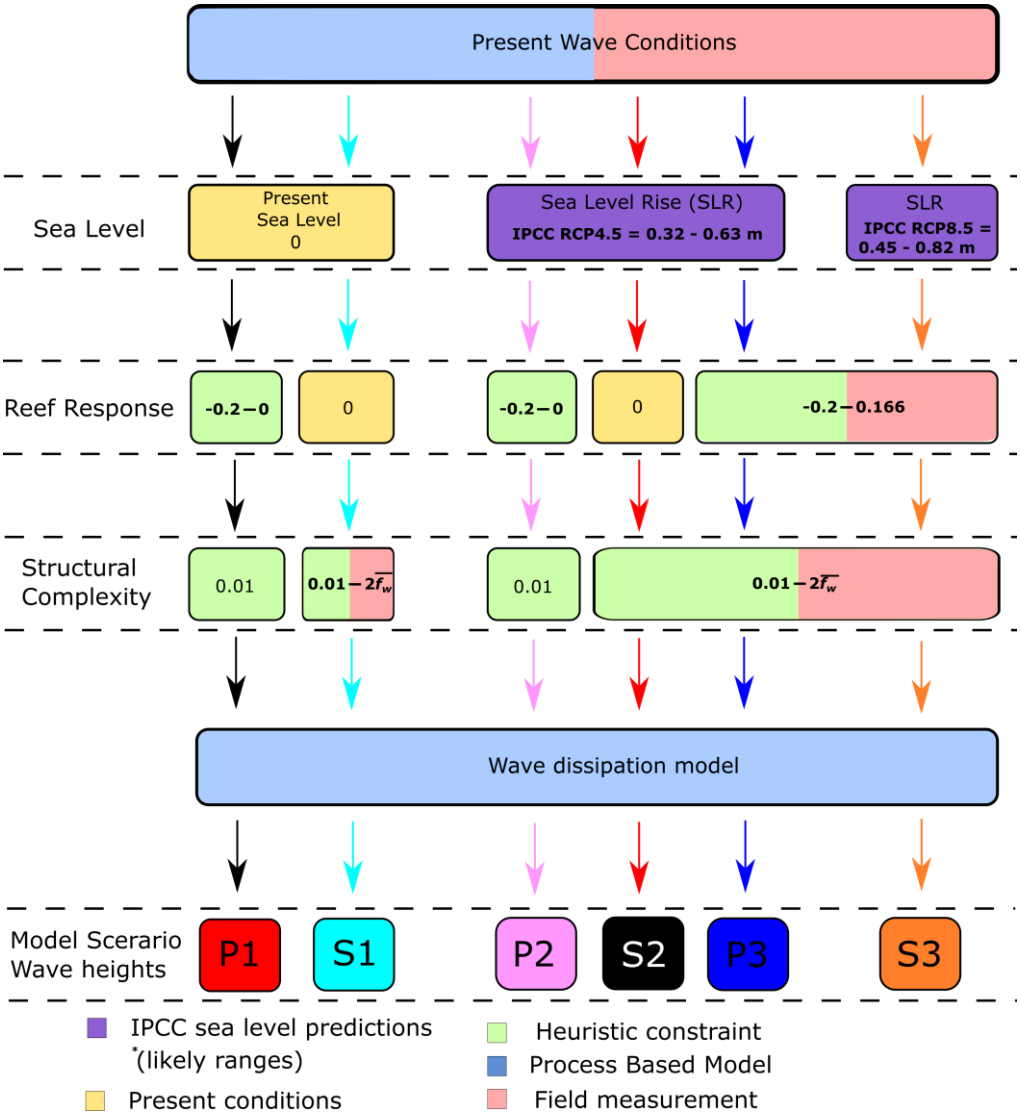

fig. S1. Schematic representation of the inputs into the wave dissipation simulations for the six scenarios (P1 to P3 and S1 to S3) described in the main text. Colouring indicates the type of data input used in the simulations. Bold values indicate the inputs that varied randomly with each Monte Carlo simulation between the reported normally distributed ranges. Sea level and reef response values are in metres from present conditions. $\overline{f_w}$ is the mean structural complexity at present for each coral reef site. $\overline{f_w}$ = 0.3, 0.11, 0.22, 0.03 for Tiahura, Temae, Ha'apiti and Teahupo'o respectively (Methods). The maximum recovery and increase in structural complexity of the reef was considered to be up to twice the present mean value ($2\overline{f_w}$). Colours for the five wave scenarios are coordinated with model results in Fig. 3.

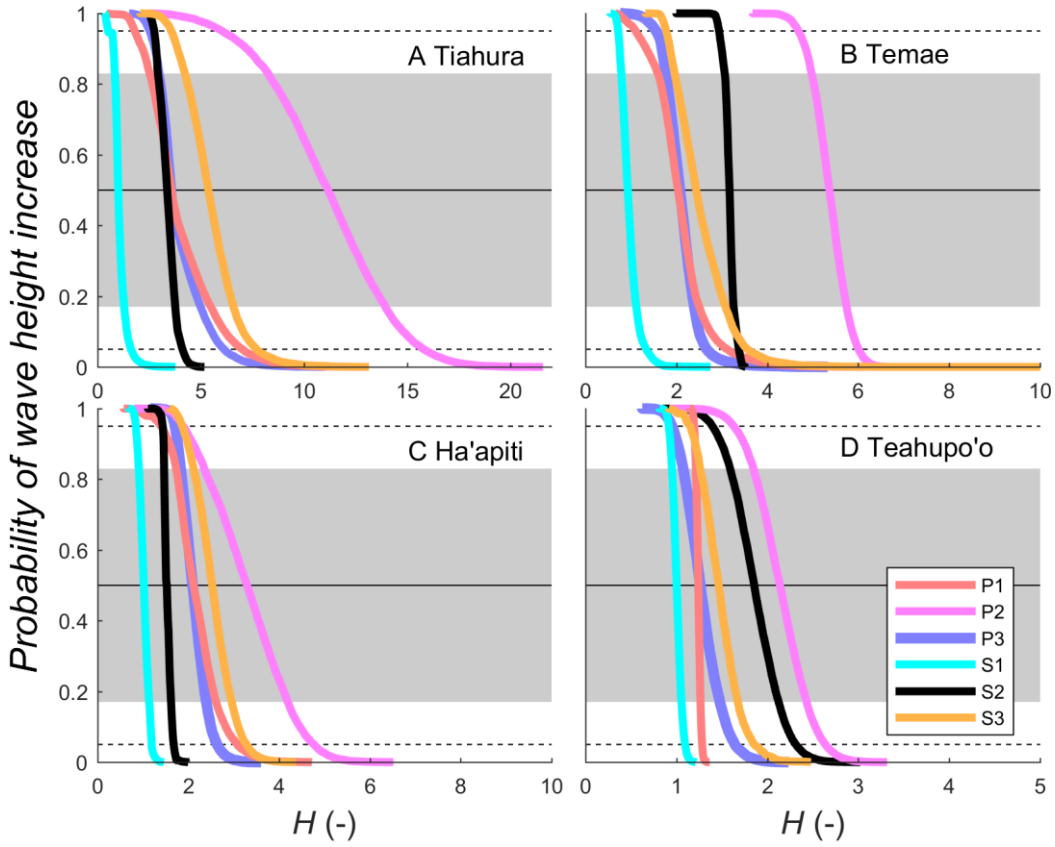

fig. S2. Changes in back-reef wave height for different scenarios and energy regimes. Results are shown for each reef site and organized by energy conditions: a) low-energy Tiahura; b) intermediate-energy Temae; c) high-energy Ha'apiti; and, d) high-energy Teahupo'o. The probability of increases in wave height (H (-)), is shown for all six scenarios (see Fig. 2). Grey shaded regions show the one standard deviation range (≈ 66% of model simulations) from the most likely result of the simulations (P = 0.5). Dashed lines show the two standard deviation range (95% of model simulations). Scenarios P1-3 from the four sites are summarized in Fig. 2 in the manuscript.

Model inputs

Bathymetric profiles.

We identified four regions of interest surrounding the wave data collection sites in Tiahura (17.482 S, 149.898 W), Temae (17.5 S, 149.757 W), Ha'apiti (17.551 S, 149.9 W) and Teahupo'o (17.868 S, 149.253 W). In these four regions, we interpolated multiple data sources to obtain seamless bathymetric datasets. The steps used in the bathymetric processing are described hereafter. In each region, we digitized or extracted point and line bathymetric

information from the sources described in table S1. All data have been referred to mean sea level using the nearby tidal datum of Papeete. For Teahupo'o, we obtained a 2x2 m bathymetric map of the shallow reefs (0 to 7m depth) from World-View 2 satellite imagery. We used the tool 'Spear Relative Water Depth' of the ENVI suite, using the near infrared, green and coastal blue bands1 of the WorldView-2 imagery and calibrating relative depths to 78 depth points digitized from SHOM map # 6657.

table S1. Sources of bathymetric data sets for Moorea and Tahiti.

Source	Scale	Extracted features
SHOM, nautical map #7305	1:25000	Bathymetric points and contours, delineation of shallow water areas in correspondence of the reef crest (-0.5m depth).
SHOM, nautical map #6657	1:12500	
SHOM, nautical map AQO_0121	1:25000	
SHOM, nautical map AQN_0121	1:50000	
Satellite-derived bathymetry (*58*)		5x5m bathymetric raster obtained from Pleiades satellite imagery, from the surface to -7m depth. Reinterpolated on a 30x30m grid point.
Satellite-derived bathymetry (Teahupoo, this study)		2x2m bathymetric raster obtained from Vorld-View 2 satellite imagery, from the surface to -7m depth. Reinterpolated on a 30x30m grid point.
Field observations and pressure transducers locations		Contours of inner reef depth, -0.5m and -0.2m; depth points from locations of pressure transducers.

All the bathymetric data presented in table S1 have been interpolated to seamless bathymetric rasters (10x10 m cell size) using the ArcMap Empirical Bayesian Kriging toolbox ((*59*), see table S2 for parameters). This technique allows harmonisation of any discrepancies that exist between datasets of different origin such as those we had available for our study sites, and produces a predicted bathymetry with a standard error estimate associated to it. These datasets allowed us to extract a representative bathymetric profile and its associated depth standard error from each area of interest (fig. S3). These profiles are those we used as input to our wave models.

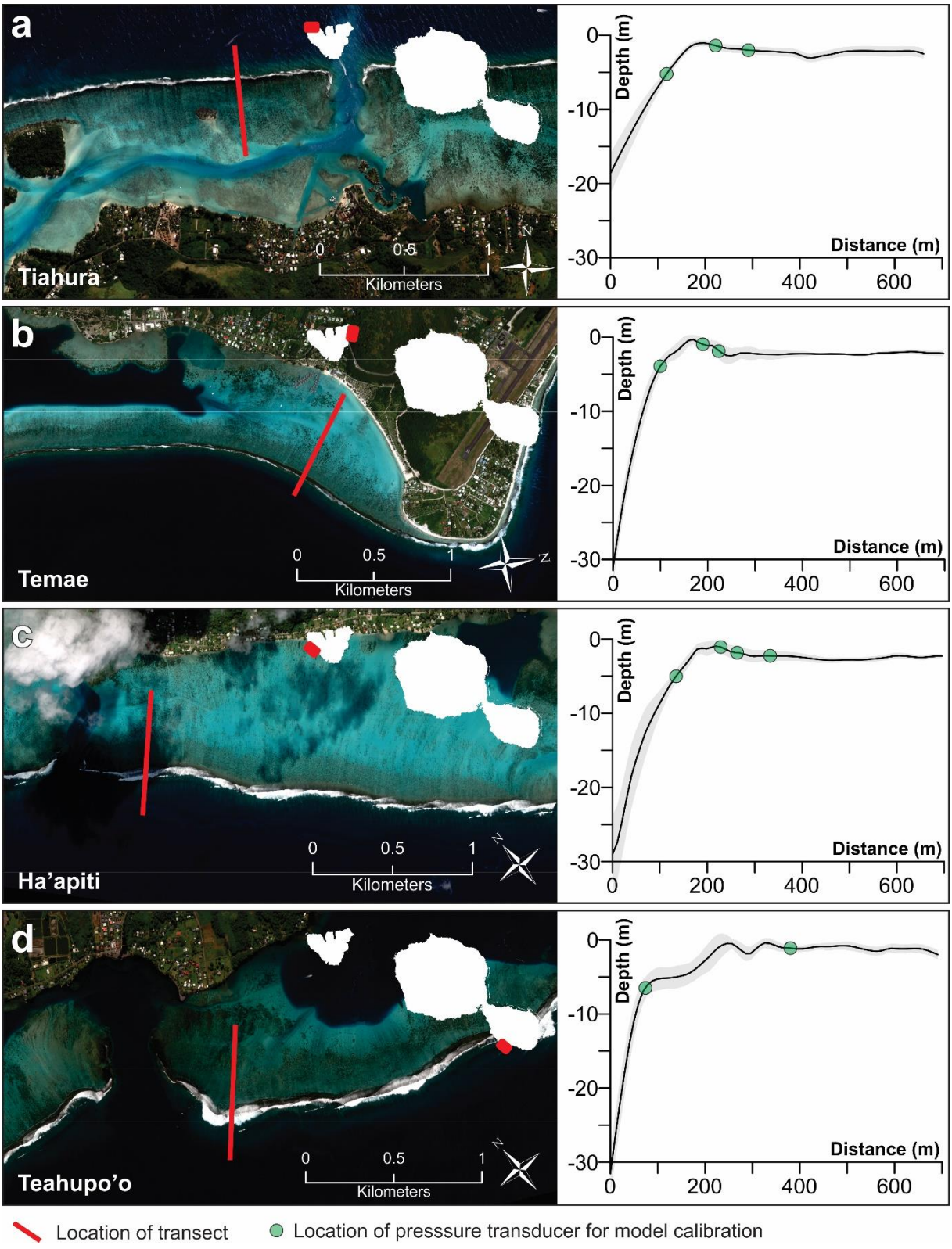

fig. S3. Locations of the cross-reef bathymetric profiles and of the wave measurements for the four reef sites in Moorea and Tahiti. (**a-d**) left panels, locations of cross-reef profiles of the four sites in Moorea and Tahiti where the wave models have been calibrated. Right panels, locations of cross-reef profiles of and of each pressure transducer used to calibrate the wave models.

Sea level change

In our wave model scenarios, we vary the sea level following predictions IPCC predictions based on the RCP scenarios 4.5 and 8.5 (*25*). In fig. S4 we show the regional signal of global mean sea level change predicted between 1986-2005 and 2081-2100. In both RCP scenarios, the average global predicted sea level change is similar to the regional sea level change predicted for Tahiti. Thus, in our scenarios (P2-3 and S2-3) we varied the sea level parameter based on the mean and likely ranges of 0.48 m (0.32 – 0.63 m) and 0.62 (0.45 – 0.82 m) for the RCP scenarios 4.5 and 8.5 respectively (fig. S4 and Methods).

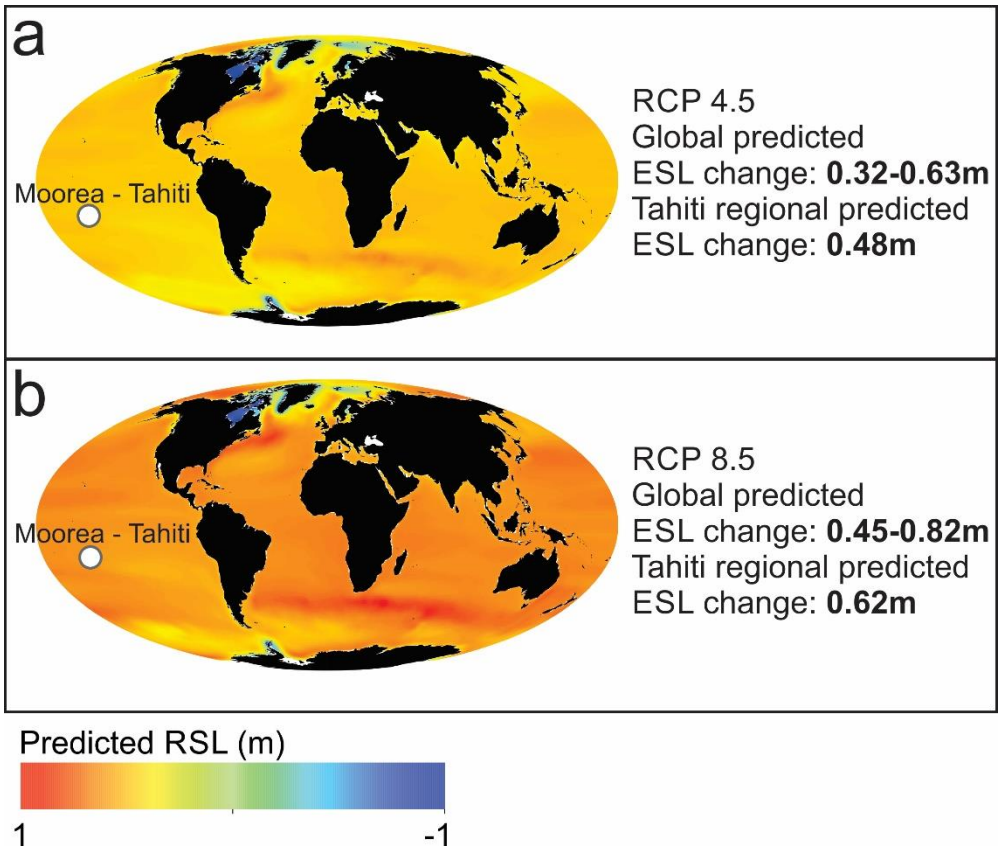

fig. S4. Global map of sea-level rise predictions by 2100 by the IPCC for the RCP4.5 and RCP8.5 scenarios. Ensemble regional relative sea level change evaluated from 21 CMIP5 models for the RCP scenarios 4.5 (**a**) and 8.5 (**b**) between 1986-2005 and 2081-2100. Note that the average predicted sea level change in Tahiti is equal to the global average.

Wave data collection

Pressure records in the surf zones of the four coral reef sites were collected during August and September 2015 and were used to calculate wave data. Over 430 hours of data were used to calibrate XBeach (Methods). The conditions measured were consistent with winter swell with waves primarily from the southwest. Greater wave heights were recorded on the exposed reefs of Ha'apiti and Teahupo'o when compared to the semi-protected environment of Temae and protected environment of Tiahura on the leeward side of Moorea (fig. S3). High wave height to water depth ratios near breakpoint were observed in both individual and time-averaged wave data and supports the breaker criterion (γ) values selected for the XBeach breaker dissipation predictions (fig. S5).

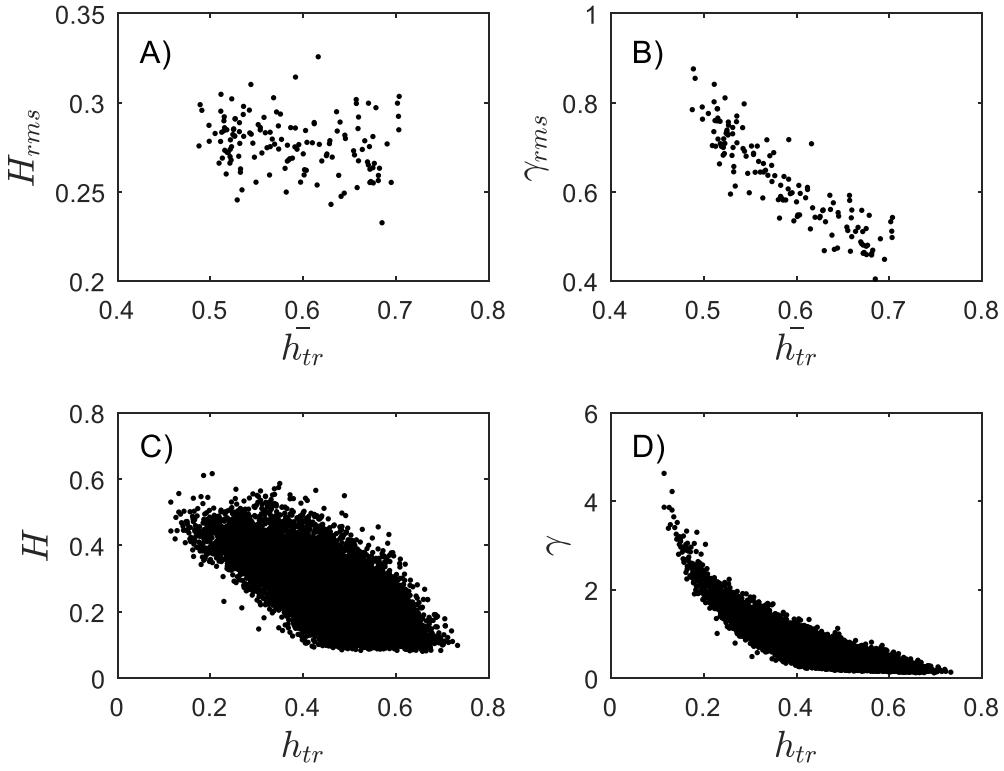

fig. S5. Example of time-averaged and individual wave heights for Tiahura near breakpoint. Example of time-averaged and individual wave heights for Tiahura near breakpoint. (**A**) shows time-averaged root-mean-square wave height (H_{rms}) compared to average water depth $(\overline{h_{tr}})$; (**B**) is the root-mean-square ratio of wave height to water depth where $\gamma_{rms} = H_{rms}/\overline{h_{tr}}$ compared to $\overline{h_{tr}}$; (**C**) and (**D**) are individual wave height (H) and the ratio of wave height to the average water to depth for individual waves (γ) for the average water depth of each wave (h_{tr}) respectively.

Model calibration

Xbeach was calibrated using pressure records measured from the surf zones of the four sites in Moorea and Tahiti (Methods). Figure S6 and S7 show the comparison and correlation between modelled and measured root-mean-square wave height. The models showed high correlation between measured and modelled waves with low root-mean-square errors as shown in Table 1 in the methods.

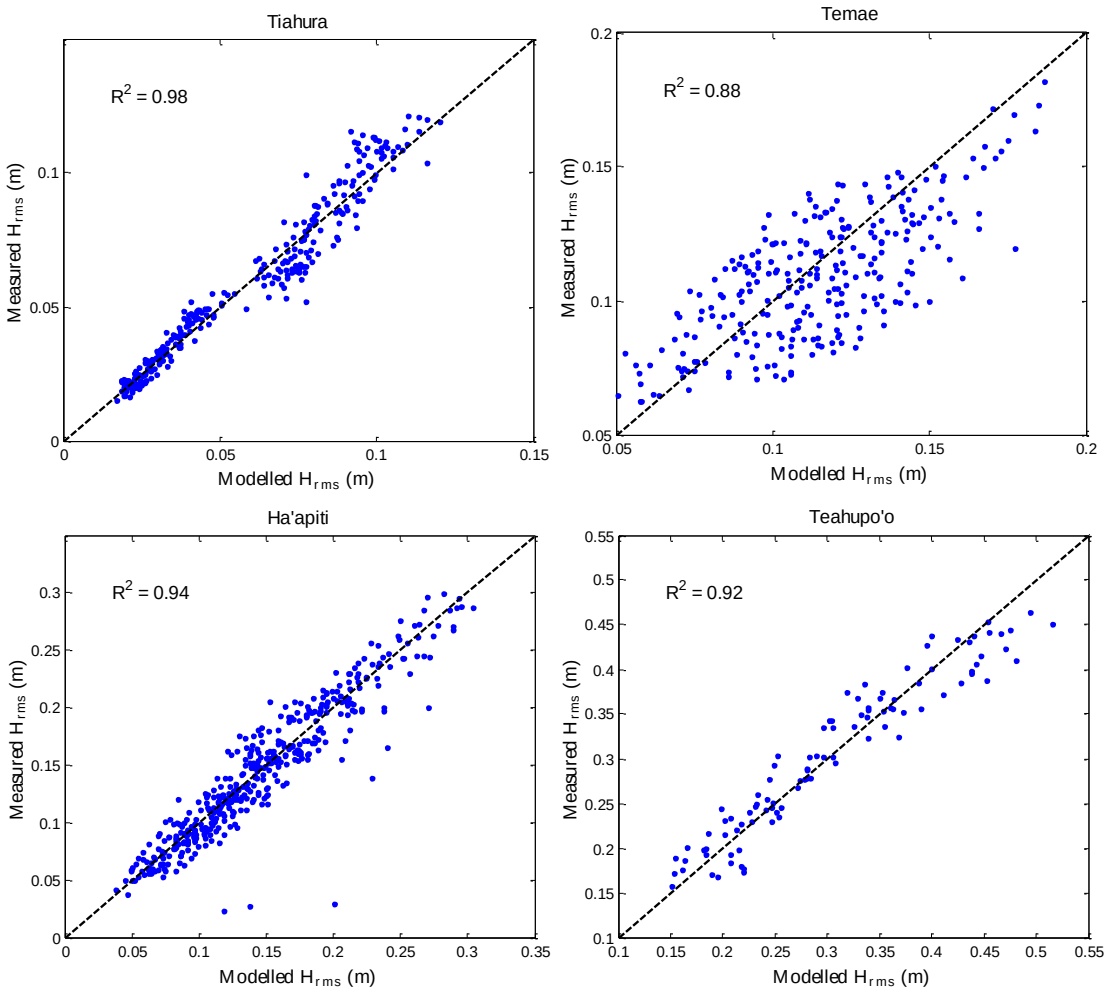

fig. S6. Comparison of the modeled and measured wave for each deployment location on the reef flats and lagoon of the four sites in Moorea and Tahiti. The dotted black line is the 1:1 ratio.

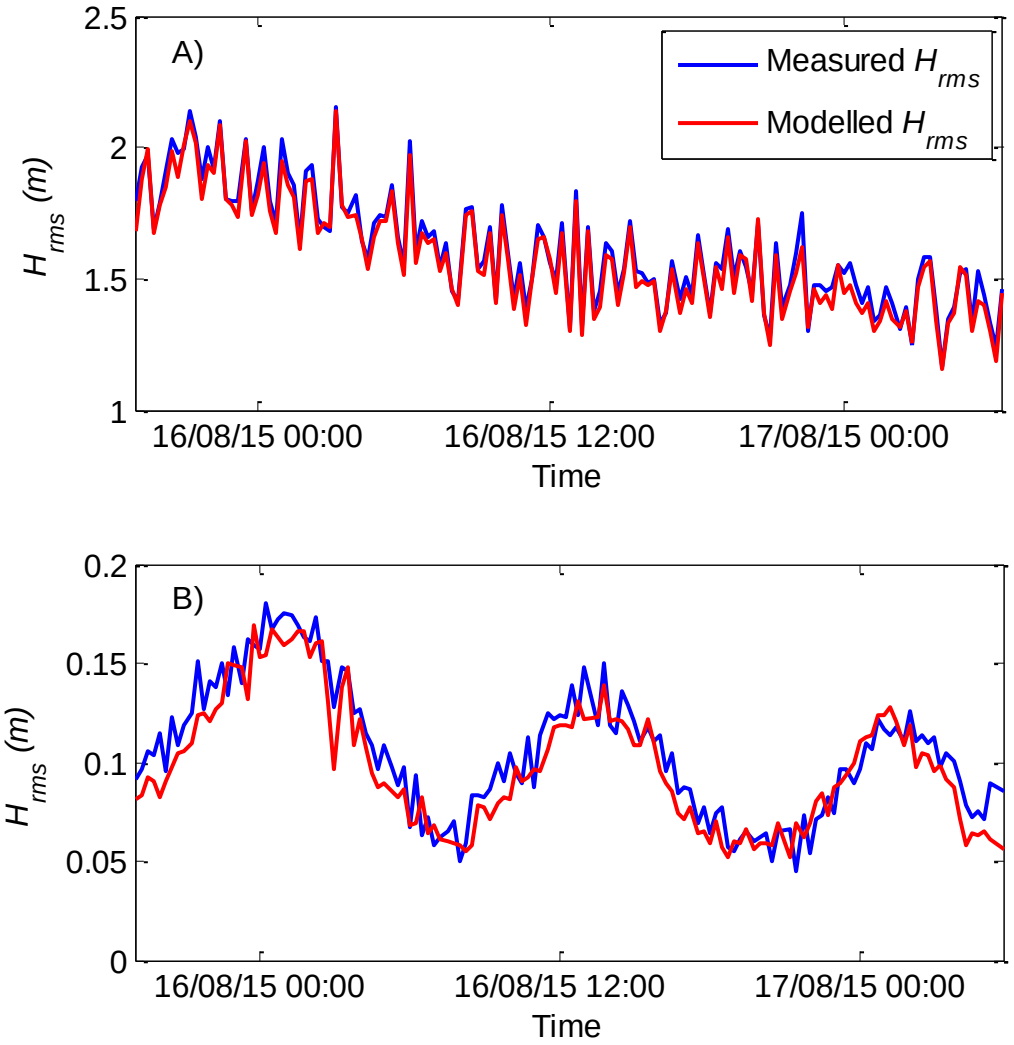

fig. S7. Example time series for Ha'apiti, Moorea. Comparison between the measured and modelled waves for: (**A**) pre-breaking waves on the fore-reef slope of Ha'apiti; and, (**B**) lagoonal wave heaights after wave dissipation on the reef crest of Ha'apiti.

Offshore wave climate

Moorea and Tahiti in French Polynesia are volcanic high islands surrounded by fringing coral reefs located in the South Pacific Ocean. Moorea and Tahiti are subject to high energy wave events from the southwest throughout most of the year particularly during winter months (fig. S8). Field sites were selected based on their exposure to the dominant swell regime. Tiahura is north facing and has the lowest annual wave energy immediately offshore (low-energy),

followed by Temae which faces southeast (moderate energy), Ha'apiti and Teahupo'o which face southwest (high-energy). Wave conditions during the measurement period were on average H_{so} = 2.05 m and T_p = 13 s, which is very similar to the long-term (1979-2013) average of H_{so} = 1.9 m and 14 s. The wave heights measured at each reef site during the deployment period were also similar to the long-term mean conditions measurement by the CRIOBE (Tiahura) and Moorea LTER (Temae and Ha'apiti, (*44*)) deployments (Methods, fig. S9). Waves were slightly larger in most locations, with the exception of Tiahura, and represents a typical southwesterly swell regime.

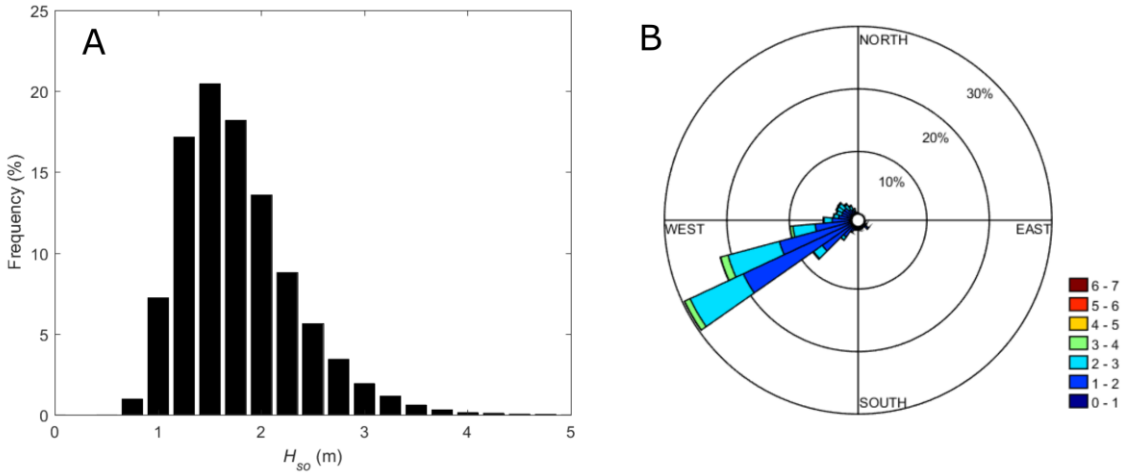

fig. S8. Summary of long-term offshore wave data (1979–2013) for Tahiti and Moorea from National Oceanic and Atmospheric Administration WAVEWATCH III (http://polar.ncep.noaa.gov/waves/index2.shtml) (150.05°W, 17.94°S). (**A**) Distribution of offshore significant wave height (H_{so}) ; (**B**) Windrose of H_{so} and wave direction.

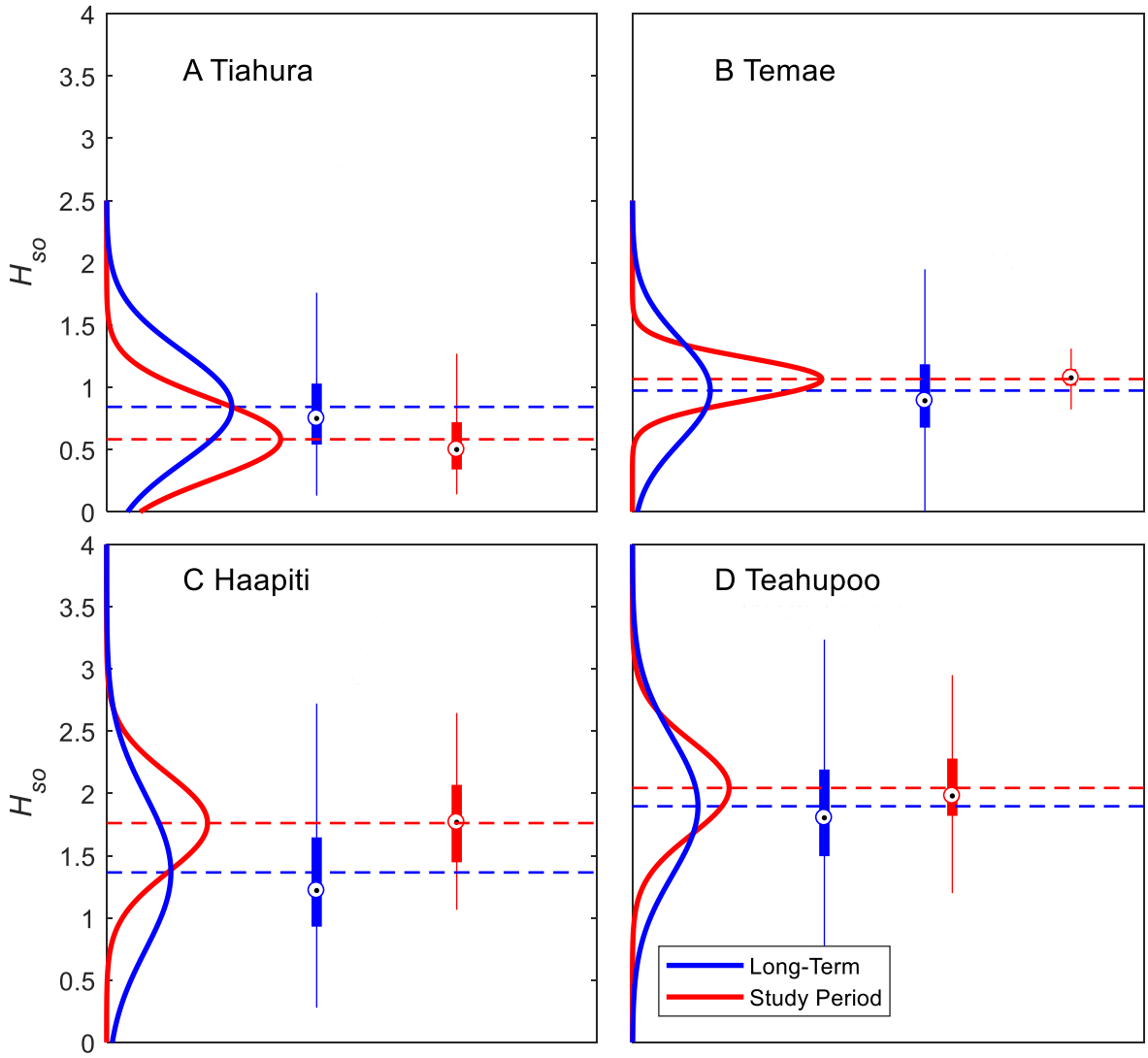

fig. S9. Comparison of the measrured offshore significant wave height (H_{so}) used to calibrate the XBeach wave model (study period) and the long-term averages from CRIOBE and Moorea LTER (*4*) measurements (long-term) for each reef site. Boxes show the interquartile range (IQR, 25th and 75th percentiles), whiskers respresent the distance of 1.5IQR from the 25th and 75th percentiles and circle markers show the median values. Dashed lines show the mean H_{so} values of which corresponds with the peak of the wave height distributions shown as solid lines.